Proc. Natl. Acad. Sci. USA
Vol. 80, pp. 1992–1996, April 1983
Genetics

Intracisternal A-particle genes as movable elements in the mouse genome

(endogenous retrovirus/insertional mutations/κ light chain genes/long terminal repeat sequence)

EDWARD L. KUFF†, ANITA FEENSTRA†, KIRA LUEDERS†, LEONARD SMITH†, ROBERT HAWLEY‡§, NOBUMICHI HOZUMI‡§, AND MARC SHULMAN§¶

†Laboratory of Biochemistry, National Cancer Institute, National Institutes of Health, Bethesda, Maryland 20205; ‡Ontario Cancer Institute and §Department of Medical Biophysics, University of Toronto, Toronto, Ontario, Canada M4X 1K9; and ¶Rheumatic Disease Unit, Wellesley Hospital, Toronto, Ontario, Canada M4Y 1J3

Communicated by Maxine Singer, December 27, 1982

ABSTRACT **We analyzed two functionally defective mouse κ light chain gene variants previously shown to contain novel insertions of repetitive DNA in their intervening sequences [Hawley, R. G., Shulman, M. J., Murialdo, H., Gibson, D. M. & Hozumi, N. (1982) *Proc. Natl. Acad. Sci. USA* 79, 7425–7429]. Heteroduplex analysis of the cloned genes shows that the insertions consist of intracisternal A-particle (IAP) genetic elements. Each insertion includes an IAP 5′ long terminal repeat (LTR) sequence and extends to a characteristic IAP internal *Bam*HI site where the IAP sequence is interrupted because the mutant genes were cloned from complete *Bam*HI digests of the cellular DNAs. Restriction enzyme mapping indicates that the 5′ LTR boundaries of the inserted IAP elements correspond closely to the previously determined rearrangement sites in the mutant genes. The IAP insertions in the two mutants can be distinguished by restriction-site differences and by the fact that one of them contains a deletion that is absent in the other. Nucleotide sequence data are presented for the LTRs of one full-length IAP gene copy randomly selected from a mouse genomic DNA library. These LTRs show many features typical of known integrated retroviral terminal repeat units, and the entire gene is bracketed by short direct repeats within the adjacent cellular DNA. Thus, the findings show that IAP genetic elements can appear in new locations in mouse cellular DNA and suggest that this may occur through a process of proviral insertion.**

In a previous study (1), κ light chain genes were isolated from two mutant mouse hybridoma cell lines defective in κ light chain production and were compared with the corresponding functional gene in the parental hybridoma line. The mutant genes were found to contain repetitive DNA elements in their intervening sequences that were not present in the intervening sequences of the wild-type κ light chain gene. Indirect evidence indicated that the insertions contained sequences related to the mouse intracisternal A-particle (IAP) genes, a group of endogenous proretroviral-like elements present in about 1,000 copies per haploid genome of *Mus musculus* (2–5).

These observations were of interest because the particles themselves, while found routinely in early mouse embryos (6–9) and abundant in the cells of many mouse tumors (10), do not have a recognized extracellular phase and have not been associated with any type of biological activity. Horizontal transmission has not been detected between cells in culture (11), and IAPs isolated from tumor cells have not proved to be infectious (10, 12). Although the isolated particles contain polyadenylylated genomic RNA species (13) and an intrinsic DNA polymerase activity (14), their endogenous reverse transcriptase reactions are remarkably inefficient in comparison to those associated with conventional replication—competent retroviruses (15, 16). Because the IAPs themselves appeared to be so severely defective, it could be questioned whether the extensive family of related genetic elements had any potential functional significance for the cell or organism.

In this paper we describe experiments that have confirmed the identity of the two κ chain gene insertions as IAP genetic elements and made it clear that the amplified family of IAP-related genes must be considered a source of insertional mutations in the mouse. Additional evidence presented here is consistent with a process of mutagenesis by proviral insertion analogous to that observed (17, 18) or indicated (19) in the case of several type C retroviruses.

MATERIALS AND METHODS

A-Particle and κ Light Chain Gene Recombinants in λ Phage. Mouse IAP genes *MIA2* and *MIA14* were representative examples of the endogenous IAP gene population selected from a BALB/c mouse embryo genomic library in λ phage Charon 4A (3, 5); these recombinants, λMIA2 and λMIA14, each contained a 7.2-kilobase-pair (kbp) IAP element plus flanking mouse DNA for total insert lengths of 16.7 and 17.3 kbp, respectively. Fragments containing the wild-type anti-2,4,6-trinitrophenyl (TNP) κ light chain gene *Tκ1* and the two mutant genes *Tκ2* and *Tκ3* (1) were cloned in λ phage Charon 28 from complete *Bam*HI digests of cellular DNAs from the respective hybridoma cell lines Sp603, igk-20, and igk-1 (20). (The insert sizes in the λTκ recombinants are shown in Fig. 2.) The nucleotide sequence of the functional gene in *Tκ1* is known (1, 21). The positions of the novel DNA insertions in *Tκ2* and *Tκ3* were established from restriction endonuclease cleavage data (1).

Heteroduplex Analysis. Recombinant phage were lysed with EDTA and alkali, and heteroduplexes were prepared and spread by the formamide technique of Davis *et al.* (22) precisely as described (5).

Nucleotide Sequence Analysis. Physical maps of *MIA2* and *MIA14* have been published (3, 5). For nucleotide sequence analysis (23) of the IAP LTRs, restriction fragments containing the terminal portions of the gene and adjacent flanking DNA were subcloned from λMIA14 into pBR322: in pMIA9, a 1.6-kbp *Hin*dIII/*Eco*RI insert included about 1.3 kbp of flanking sequence, the 5′ IAP LTR, and 15 bp of internal IAP sequence; and in pMIA6, a 1.0-kbp *Hin*dIII fragment contained 450 bp of 3′ internal IAP sequence, the 3′ LTR, and 200 bp of downstream flanking DNA. Appropriately cut fragments (see Fig. 4 legend) were labeled at their *Pst* I ends with cordycepin 5′-[α-

The publication costs of this article were defrayed in part by page charge payment. This article must therefore be hereby marked "*advertisement*" in accordance with 18 U. S. C. §1734 solely to indicate this fact.

Abbreviations: LTR, long terminal repeat; IAP, intracisternal A particle; kbp, kilobase pair(s); TNP, 2,4,6-trinitrophenyl.

^{32}P]triphosphate and terminal deoxynucleotidyltransferase (24) or at *Alu* I and *Eco*RI ends with [γ-^{32}P]ATP and T4 polynucleotide kinase (25).

Restriction Site Analysis. A *Kpn* I/*Msp* I fragment from pMIA9 (see Fig. 3) was labeled with [α-^{32}P]dATP by nick-translation (26) to use as a hybridization probe for IAP LTR sequences. A general IAP sequence probe was prepared by similarly labeling the 5.2-kbp *Hin*dIII/*Eco*RI fragment from the previously described recombinant plasmid pMIA1 (3). DNA from the $\lambda T\kappa$ recombinants was digested with restriction enzymes (New England BioLabs), and the digests were electrophoresed in 1.4% or 2.0% agarose gels. Ethidium bromide-stained fragments were transferred from agarose gels to diazotized aminophenyl thioether paper (27) by using the basic method of Alwine *et al.* (28) as elaborated by the manufacturer (Schleicher & Schuell). Hybridizations were carried out as described (3, 5).

RESULTS

Identification of IAP Homology Regions in Mutant κ Light Chain Genes. When phage DNAs carrying the wild-type and mutant κ light chain genes were applied to nitrocellulose filters and hybridized with a radiolabeled probe prepared from cloned mouse IAP sequences (3), both mutant gene recombinants $\lambda T\kappa 2$ and $\lambda T\kappa 3$ gave strong positive reactions, while the recombinant containing the wild-type gene $\lambda T\kappa 1$ was negative (data not shown).

Heteroduplexes were then prepared between $\lambda T\kappa 2$ and $\lambda T\kappa 3$ and two recombinants, λMIA2 and λMIA14, containing representative endogenous 7.2-kbp IAP genes in appropriate orientations (3). An example of each pairing is shown in Fig. 1 *A* and *B* together with drawings that indicate the individual DNA strands in the heteroduplexes and the known positions of the IAP gene sequences in the λMIA partners (3). Fig. 1*C* shows the portions of the IAP gene which are represented in $\lambda T\kappa 2$ and $\lambda T\kappa 3$. In both cases, the homology region appears to include the 5′ IAP LTR. The homologous segment in $\lambda T\kappa 2$ is colinear with the IAP gene in λMIA2 over a distance of about 4.3 kbp. In $\lambda T\kappa 3$, the IAP homology region measures 2.3 kbp in length; however, it contains a deletion of 2.1 kbp with respect to the complete IAP gene in λMIA14 (asterisks in Fig. 1*B*), and when this is taken into account, the overall IAP map distance spanned by the *Tκ3* homology region is the same as that seen in *Tκ2*. In both cases, the 3′ end of the IAP homology region falls at a position corresponding to a *Bam*HI site typically located 4.2 kbp from the 5′ end of the IAP genes (Fig. 1*C*). This is consistent with the fact that the $\lambda T\kappa$ recombinants were prepared from complete *Bam*HI digests of the respective cellular DNAs (1). Deleted forms of IAP genes have been described (4, 5), and Shen-Ong and Cole (31) have distinguished a particular "Type II" subclass of IAP genetic elements that contain deletions similar to that seen in the *Tκ3* IAP segment. However, it is not clear that the segment in *Tκ3* is actually representative of the type II group because the heteroduplex analysis failed to reveal the short insertion that characteristically adjoins the deletions in these genes. The question is of interest because of an indication that type II genes were increased in number in the DNA of a BALB/c myeloma cell line as compared to the germ-line DNA (31).

The results of the heteroduplex analysis were combined in Fig. 2 with previous mapping data (1) to show the spatial relationships between the inserted IAP sequences and the κ light chain gene sequences in $\lambda T\kappa 2$ and $\lambda T\kappa 3$. The IAP sequences clearly correspond in position, orientation, and general size to the segments of foreign DNA as they have been described (1). However, the heteroduplex measurements, with standard errors of 300 bp or more were of limited value in locating the 5′ boundaries of the IAP sequences with respect to the rearrangement sites in the mutant genes (Fig. 2). Precise information on this point was important in considering possible mechanisms for insertion of the IAP elements; for example, a clean transition from light chain gene to LTR sequence would be consistent with a proviral insertion, whereas the presence of additional (non-IAP) sequence at the junction points might

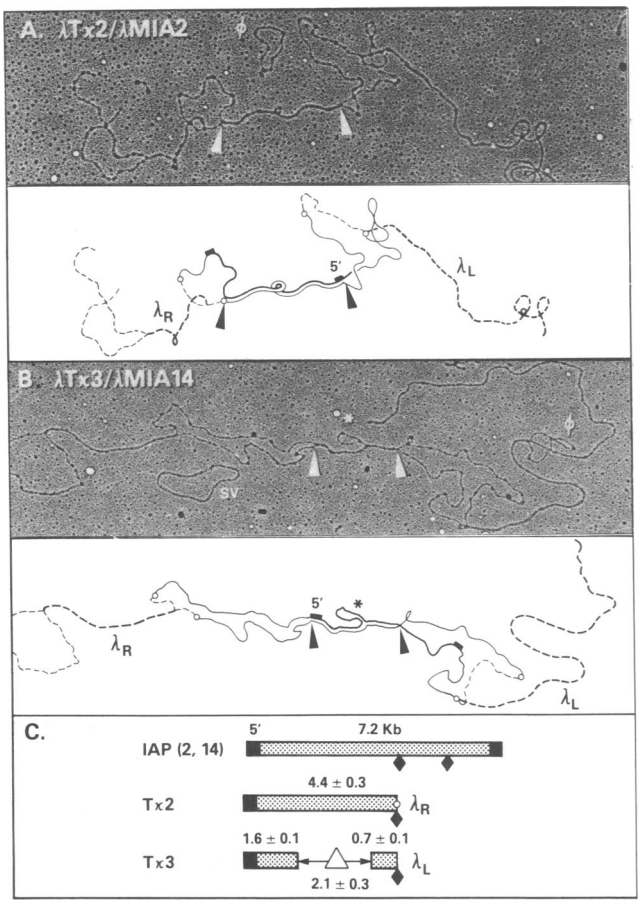

FIG. 1. Heteroduplex analysis of the IAP sequences in two mutant κ light chain genes. Recombinants $\lambda T\kappa 2$ and $\lambda T\kappa 3$ contained the mutant genes within *Bam*HI fragments cloned into λ phage Charon 28 (1). Heteroduplexes were formed with λMIA2 and λMIA14, which contain 7.2-kbp IAP genes in known positions and appropriate orientations (3); these genes and adjacent flanking sequences had been cloned into Charon 4A from a partial *Eco*RI digest of BALB/c embryo DNA. (*A*) Electron micrograph and drawing of a representative heteroduplex between $\lambda T\kappa 2$ and λMIA2. A 4.4-kbp region of homology is delimited by the pointers. In the drawings, the mouse sequence elements are indicated by continuous lines, and the phage arms are indicated by heavy or light broken lines that signify paired or unpaired strands, respectively. Junction points between the mouse DNA and phage arms are indicated by open circles; the contributions of the phage arms to the two large single-stranded bubbles were calculated from published data on the structures of the Charon 4A and 28 vectors (29, 30). The known position of the IAP sequences on the λMIA2 strand is indicated by the heavy solid line, with short solid boxes representing the IAP LTRs. (*B*) Similar representations of a heteroduplex between $\lambda T\kappa 3$ and λMIA14. The 2.3-kbp homology region (between pointers) shows a single-stranded loop (*) indicative of a deletion within the IAP homology region in $\lambda T\kappa 3$. SV and ϕ are simian virus 40 and ϕX174 DNA molecules added as double- and single-stranded size markers, respectively. (*C*) Diagrams showing a "standard" 7.2-kbp IAP gene and the homologous regions which are represented in *Tκ2* and *Tκ3*. The homology regions in both *Tκ2* and *Tκ3* appear to include a 5′ LTR (■) and extend to a position corresponding to one of the characteristic *Bam*HI sites (◆) in the IAP gene (3, 5). The homology segment in $\lambda T\kappa 3$ contains a deletion (△) of 2.1 kbp with respect to the intact IAP sequence. Dimensions shown for the *Tκ2* and *Tκ3* homology regions are the means and standard errors derived from measurements of 20 heteroduplex molecules.

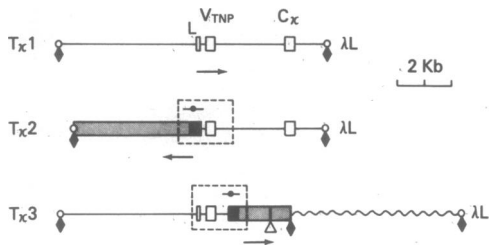

FIG. 2. Relationships between the κ light chain coding regions *L*, V_{TNP} (variable segment of the κ_{TNP} gene), and C_κ (constant region gene of the κ chain) (open boxes) and the IAP homology regions (stippled bars with solid LTR regions) in the λTκ recombinants. Junctions of the mouse sequence with the phage arms (○) and the known positions of *Bam*HI restriction sites (◆) are indicated. The insert in λTκ3 contains a second *Bam*HI fragment of unrelated mouse sequence (wavy line), presumably the result of a packaging artefact during preparation of the recombinant library. Arrows, 5′ to 3′ orientation of the sequence elements (the IAP components in *Tκ2* and *Tκ3* lie in opposite orientations); △, location of the deletion in the IAP segment of *Tκ3*. The positions of the light chain gene elements were known from previous studies (1). —●—, Locations of the 5′ boundaries of the IAP components in *Tκ2* and *Tκ3* as determined from the heteroduplex data (means and standard error of the measurements). The actual placement of the IAP sequences is based on restriction site analysis (see Fig. 3) of the regions enclosed by the broken lines.

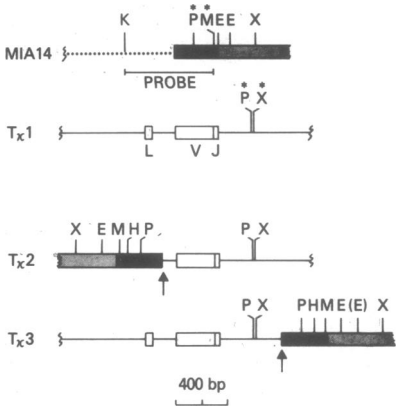

FIG. 3. Restriction enzyme analysis of the junction regions between κ light chain sequences and the IAP elements in *Tκ2* and *Tκ3*. (*Upper*) Relevant restriction endonuclease sites near the 5′ end of the IAP gene contained in *MIA14* (stippled bar with solid LTR region) and near the *L–V* (variable)–*J* (joining) exon regions (open boxes) in the wild-type κ light chain gene cloned in *Tκ1*. Mouse flanking sequences 5′ to the IAP gene are indicated by a dotted line. The restriction enzymes were: K, *Kpn* I; P, *Pst* I; M, *Msp* I; E, *Eco*RI; and X, *Xba* I. The restriction sites were mapped previously (1, 3, 5). *, Sites located from nucleotide sequence data as well as enzyme cleavage. (*Lower*) Positions of the restriction sites in the mutant light chain genes. DNAs were prepared from λTκ2 and λTκ3 and digested with *Xba* I alone or in conjunction with the other enzymes. One-microgram portions of the digested DNAs were electrophoresed in 1.4 or 2.0% agarose gels, and the fragments were transferred to *o*-diazophenyl thioether paper. The blots were hybridized with a ^{32}P-labeled probe consisting of the *Kpn* I/*Msp* I fragment from *MIA14* (*Upper*). The mouse flanking sequences within this fragment are unique to the *MIA14* IAP gene (unpublished data). The probe is specific for LTR sequence in the present experiments because the IAP segments in both *Tκ2* and *Tκ3* could be distinguished clearly from the *MIA14* gene on the basis of their restriction patterns as well as the deletion in the *Tκ3* insertion. The observed sizes (in bp) of the LTR-reactive fragments in digests of λTκ2 DNA were: X alone, 1.40; X/P, 0.88 and 0.52; X/H, 1.00 and 0.37; X/M, 1.06; and X/E, 1.20. For λTκ3 DNA, the corresponding fragment sizes were: X alone, 1.00; X/P, 0.62 and 0.33; X/H, 0.46 (doublet); X/M, 0.55; and X/E, 0.67. With these data and the approximate positions of the IAP and κ chain elements already determined by heteroduplex analysis, the restriction sites were ordered (*Lower*). The segments of LTR sequence were then positioned with respect to the *Pst* I and *Msp* I sites as they are in the reference IAP gene *MIA14*. Arrows, sites of transition between wild-type κ light chain sequence and foreign DNA sequence as determined by restriction enzyme mapping (1). In the case of *Tκ3*, (E) indicates an *Eco*RI site that was found previously (1) but was not observable with our present probe.

suggest some other mode of transposition. More detailed information on the transition regions in *Tκ2* and *Tκ3* (stippled boxes in Fig. 2) was obtained by the restriction enzyme analysis shown in Fig. 3.

Localization of A-Particle LTRs by Restriction Enzyme Analysis of Mutant κ Light Chain Genes. Fig. 3 *Upper* shows relevant restriction sites near the L–$V_{TNP}J_5$ region of the wild-type κ light chain gene in *Tκ1* (1, 21) and in and around the 5′ LTR of IAP gene *MIA14* (3, 5). The closely spaced *Pst* I and *Xba* I sites to the right of the variable region coding sequence *V* in *Tκ1* are known to be retained in both *Tκ2* and *Tκ3* (1) and were used as reference sites for mapping. The 5′ LTR of *MIA14* (see below) is similar in size (about 340 bp) to the LTRs of other isolated IAP genes (32) and contains a highly conserved *Pst* I site about 150 bp from its 5′ boundary. Other characteristic features of IAP genes are the *Msp* I site towards the 3′ end of the LTR and the *Eco*RI and *Xba* I sites located in the body of the IAP gene, 300 bp and 500 bp, respectively, from the *Pst* I site in the 5′ LTR (5). The *MIA14* 5′ LTR lacks a *Hin*dIII site, which is found near the *Pst* I site in many other IAP genes (5). In addition, the *Eco*RI site just outside the boundary of the 5′ LTR in *MIA14* is not a recognized common feature of other IAP genes.

DNAs from λTκ2 and λTκ3 were digested with *Xba* I alone or in combination with other restriction endonucleases. The electrophoretically fractionated fragments were transferred to *o*-diazophenyl thioether paper and hybridized with a probe for IAP LTR sequences (Fig. 3 *Upper*). *Xba* I digestion of *Tκ2* and *Tκ3* DNA yielded single reactive fragments of 1.4 and 1.0 kbp, respectively (no reaction was seen with digests of *Tκ1* DNA). Two reactive fragments of nearly equal intensity were found in the combined *Xba* I/*Pst* I digests of each mutant gene: these were 880 and 520 bp in size in the *Tκ2* digest and 620 and 330 bp in the case of *Tκ3*. These and additional data (see the legend to Fig. 3) established the restriction maps and the putative positions of LTR sequences in the rearranged light chain genes as shown in Fig. 3 *Lower*. If these LTRs are assumed to be the same size as those found in the reference IAP genes *MIA14*, their 5′ boundaries map rather precisely to the rearrangement sites previously determined by restriction mapping of *Tκ2* and *Tκ3* (1) and indicated by arrows in Fig. 3 *Lower*—i.e., the IAP insertions would appear to have brought with them little or no additional flanking sequence.

The three IAP gene segments shown in Fig. 3 could all be distinguished from one another on the basis of their restriction maps. Thus, *MIA14* and the inserted IAP gene in *Tκ2* each contained the conserved *Msp* I, *Eco*RI, and *Xba* I sites at 160, 300, and 500 bp, respectively, from their LTR *Pst* I site; however, they differed with respect to a *Hin*dIII site present in the *Tκ2* LTR and a second *Eco*RI site in *MIA14*. The LTR in *Tκ3* contained a *Hin*dIII site in the same position as that in *Tκ2*, but this gene differed from both of the others in the distance between its *Pst* I and *Xba* I sites (640 bp) and in the placement of its two *Eco*RI sites. These differences, together with the major deletion found in the IAP segment in *Tκ3* (Fig. 1) strongly indicate that separate IAP genetic units were involved in the two insertion events.

Clarification of the insertion mechanism will depend ultimately on detailed knowledge of the nucleotide sequence across both junction regions between the IAP and light chain elements in the mutant genes and comparison of these sequences

with those of other IAP LTRs. Data on the mutant genes are not yet available. Meanwhile, however, the sequences of the LTRs from the IAP gene *MIA14* were determined and, as shown below, they exhibit a number of the features specifically associated with the formation and insertion of provirus copies of conventional replication-competent retroviruses.

Nucleotide Sequence of LTRs from a Complete IAP Genetic Unit. The overall length of the LTR sequence (Fig. 4*A*) was 338 bp. Eight positions near the *Pst* I in the 3′ LTR were not determined. However, the two sequences agreed in 323 of the 330 positions that were determined for both LTRs. The observed single-base differences could have arisen by random mutations since this gene copy was generated during the evolution of *Mus musculus* (5).

Although R-looping studies show that the *MIA14* gene is colinear with 35S IAP genomic RNA (5), we do not know whether this particular IAP copy is functionally competent. In

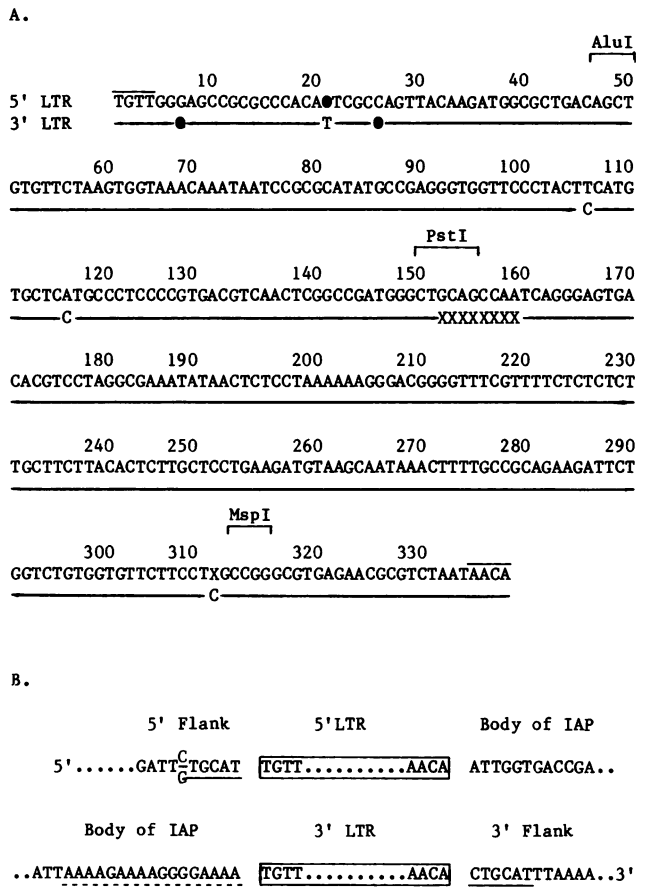

FIG. 4. The nucleotide sequence of the LTRs (*A*) and immediately adjacent regions (*B*) in the IAP gene *MIA14*. (*A*) Positions are numbered from the 5′ end of the LTR sequences. For the 5′ LTR, sequence was determined in both directions from the *Pst* I site at positions 150–155, in a 3′ direction from an *Alu* I site at positions 47–50, and in a 5′ direction from an *Eco*RI site within the IAP gene but just to the right of the LTR (see Fig. 3). The 3′ LTR sequence was determined in both directions outward from the *Pst* I site; the nucleotides corresponding to positions 152–159 in the 5′ LTR were not determined (X). In *A*, agreement between the individually determined sequences is indicated by a horizontal line in the 3′ LTR sequence; nucleotide differences or open positions (●) are also shown on the 3′ sequence, except at position 21, where an open position appeared in the 5′ LTR sequence. Both LTR sequences end in a 4-bp inverted repeat (solid overline). In *B*, 17-bp polypurine stretch is located within the IAP gene immediately upstream from the 3′ LTR (broken underline). A 5- or 6-bp sequence (solid underline) is repeated in the immediate flanking regions; one nucleotide in the 5′ sequence could not be determined unambiguously because of secondary structure hindrance.

any event, its LTRs share the following properties with the proviral LTRs of known infectious retroviruses (33): (*i*) short (4 bp) inverted repeats at the ends of each LTR; (*ii*) a long (17 bp) polypurine stretch immediately upstream from the 3′ LTR; (*iii*) an A+T-containing sequence reminiscent of the eukaryotic "TATAA" box (34) at positions 184–191; and (*iv*) the canonical polyadenylylation signal A-A-T-A-A-A (35) at positions 265–270. A possible poly(A) acceptor sequence, C-A (36), is found at positions 280 and 281. The relative positions of these signal sequences are characteristic of their arrangement in conventional retroviral LTRs (33). The reference *Pst* I shown in Fig. 3 is located at positions 150–155. The position of the putative TATAA box is consistent with the results of previous studies (5, 37), which mapped the 5′ end of IAP-associated RNAs to a position just downstream from this *Pst* I site. Twelve nucleotides beginning at position 337 of the 5′ LTR and extending into the body of the IAP gene are identical in 11 positions with 12 nucleotides that begin near the end of the 5′ LTR of the avian sarcoma virus and extend into the tRNA primer binding site of that virus (38). The tRNA binding sites in Rous sarcoma virus and other replication-competent retroviruses are typically 18–20 bp long (33). Additional sequence data are required to determine whether a similar-size site occurs in the IAP gene.

The integration of known free proviruses is accompanied by loss of two nucleotides from the 5′ end (U3 region) of the 5′ LTR and two from the 3′ end (U5 region) of the 3′ LTR (33). The original sequence of the inverted repeats can be deduced from that of the integrated provirus, however, because these two nucleotides appear just preceding the 3′ LTR and (in inverted complementary form) just following the 5′ LTR. From the data in Fig. 4*B*, the reconstructed sequence of the inverted repeats in the LTRs of a hypothetical *MIA14* free provirus would be

5′ . . . A-A*T-G-T-T . . . (IAP) . . . A-A-C-A*A-T . . . 3′,

where asterisks indicate the apparent integration sites. The sequence A-A*T-G is common to both avian and mammalian proviral LTRs, and T appears in position 5 of the avian virus LTR (33).

Short duplications of the target site sequence are characteristically associated with integration of retroviral DNA copies (33) as well as transposable elements in lower organisms (39, 40). In the case of *MIA14*, we observed a 6-bp direct repeat of flanking mouse sequences adjacent to the two LTRs (Fig. 4*B*).

DISCUSSION

The findings in this and a previous report (1) provide direct evidence that IAP genetic units can act as movable elements in the mouse genome. The insertions in *Tκ2* and *Tκ3* can be distinguished from one another on the basis of their restriction maps and the presence of a major deletion in one of them; therefore, it is likely that they represent two different members of this multigene family. Our data suggest that, in both instances, the IAP components were inserted close to or at their LTR boundaries. Preliminary sequence data for the junction region in *Tκ2* indicate a clean transition from κ chain gene to IAP LTR sequence; the first 35 nucleotides after the junction have been determined and found to have a 91% homology with the *MIA14* LTR sequence (Fig. 4) between positions 2 and 38 (unpublished data). Should this result prove the rule for both the 5′ and 3′ junctions of the inserted elements in *Tκ2* and *Tκ3*, and should the analysis also reveal short direct repeats of the target site sequences, we would conclude that the IAP elements in the mu-

tant genes represent authentic proviral insertions. However, we still might be unable to distinguish between the transposition of IAP gene copies already present in the genomic DNA and the insertion of new proviral forms generated from IAP-associated RNA in the particle-producing hybridoma cells.

The distinction is important because transpositions that do not involve an RNA intermediate (39, 40) might be expected with comparable frequency in both IAP-positive and IAP-negative cells, whereas cycles of reverse transcription and proviral insertion would clearly be favored in particle-producing cells. Although direct evidence is lacking, the second possibility seems more likely to us because it involves a well-established mechanism, whereas the alternative—the precise transposition of an integrated retroviral gene copy—has not yet been demonstrated. Free proviral forms have not been found when searched for in IAP-rich myeloma (31) or neuroblastoma (unpublished data) cells; however, a small but functionally significant population could well have escaped detection in these cases, and it may be useful to carry out a further search in the Sp603 cell line in which the mutant κ chain genes arose. Evidence for an RNA intermediate might be obtained by detailed structural comparisons of the *Tκ2* and *Tκ3* insertions with the IAP-associated RNA species present in the respective cell lines.

We have searched the wild-type κ light chain nucleotide sequence (1, 21) on either side of the IAP target sites in *Tκ2* and *Tκ3* for possible homologies with the LTR sequence. Short stretches of partial homology were found, but none that obviously could have served to align an incoming provirus in the precise positions where the recombinations actually occurred. If the IAP insertions represented in *Tκ2* and *Tκ3* do indeed represent random attacks, then one might question whether similar events are not occurring elsewhere in the genome of the hybridoma cells and, by extension, in the genomes of other IAP-producing cells. In this way, the IAP gene pool might provide a significant source of genetic variability in the many mouse tumors where abundant intracisternal particles are known to occur (10). The new insertions in *Tκ2* and *Tκ3* were both associated with defective expression of the κ light chain gene products (1). It would be interesting to examine IAP-producing cell lines for spontaneous variants in other selectable traits and determine whether any of these represent a similar kind of insertional mutation. Insertions of exogenous proviruses have been shown to promote the expression of nearby cellular oncogenes (17), and the possibility must be considered that IAP genetic elements could have the same effect on occasion.

The present results are relevant to the possible amplification mechanism(s) by which the IAP genes have achieved a copy number of 1,000 or more per haploid genome in *Mus musculus* DNA. The fact that one randomly chosen endogenous IAP copy shows so many hallmarks of a proviral insertion and the direct demonstration that IAP elements can appear in new locations in the cellular DNA together suggest that amplification over an evolutionary time scale could result from the occasional insertion of new proviral copies into the germline DNA. Such a mechanism would be consistent with, and facilitated by, the observed expression of IAPs in mouse oocytes and preimplantation embryos (6–9). The insertion of new IAP copies into germ-line DNA could give rise also to specific mutations, in a manner analogous to the coat-color mutation associated with integration of an ecotropic murine leukemia virus genome (19).

We thank Bruce Paterson for aid in some aspects of the nucleotide sequence analysis and Jean Regan for her skilled assistance in preparation of the manuscript. This work was supported by grants from the Medical Research Council of Canada, the National Cancer Institute of Canada, the University of Toronto, the Arthritis Society of Canada, and the Allstate Foundation. R.G.H. was supported by a studentship of the Medical Research Council of Canada.

1. Hawley, R. G., Shulman, M. J., Murialdo, H., Gibson, D. M. & Hozumi, N. (1982) *Proc. Natl. Acad. Sci. USA* **79**, 7425–7429.
2. Lueders, K. K. & Kuff, E. L. (1977) *Cell* **12**, 963–972.
3. Lueders, K. K. & Kuff, E. L. (1980) *Proc. Natl. Acad. Sci. USA* **77**, 3571–3575.
4. Ono, M., Cole, M. D., White, A. T. & Huang, R. C. (1980) *Cell* **21**, 465–473.
5. Kuff, E. L., Smith, L. A. & Lueders, K. K. (1981) *Mol. Cell. Biol.* **1**, 216–227.
6. Callarco, P. G. & Szöllösi, D. (1973) *Nature (London) New Biol.* **243**, 91–93.
7. Chase, D. G. & Pikó, L. (1973) *J. Natl. Cancer Inst.* **51**, 1971–1975.
8. Biczysko, W., Pienkowski, M., Solter, D. & Koprowski, H. (1973) *J. Natl. Cancer Inst.* **51**, 1041–1050.
9. Yotsuyanagi, Y. & Szöllösi, D. (1981) *J. Natl. Cancer Inst.* **67**, 677–685.
10. Kuff, E. L., Lueders, K. K., Ozer, H. L. & Wivel, N. A. (1972) *Proc. Natl. Acad. Sci. USA* **69**, 218–222.
11. Minna, J. D., Lueders, K. K. & Kuff, E. L. (1974) *J. Natl. Cancer Inst.* **52**, 1211–1217.
12. Kuff, E. L., Wivel, N. A. & Lueders, K. K. (1968) *Cancer Res.* **28**, 2137–2148.
13. Paterson, B. M., Segal, S., Lueders, K. K. & Kuff, E. L. (1978) *J. Virol.* **27**, 118–126.
14. Wilson, S. H., Bohn, E. W., Matsukage, A., Lueders, K. K. & Kuff, E. L. (1974) *Biochemistry* **13**, 1087–1094.
15. Wong-Staal, F., Reitz, M. S., Jr., Trainor, C. D. & Gallo, R. C. (1975) *J. Virol.* **16**, 887–896.
16. Yang, S. S. & Wivel, N. A. (1976) *Biochim. Biophys. Acta* **447**, 167–174.
17. Neel, B. G., Hayward, W. S., Robinson, H. L., Fang, J. & Astrin, S. M. (1981) *Cell* **23**, 323–334.
18. Varmus, H. E., Quintrell, N. & Ortiz, S. (1981) *Cell* **25**, 23–36.
19. Jenkins, N. A., Copeland, N. G., Taylor, B. A. & Lee, B. K. (1981) *Nature (London)* **293**, 370–374.
20. Köhler, G. & Shulman, M. J. (1980) *Eur. J. Immunol.* **10**, 467–476.
21. Max, E. E., Maizel, J. V., Jr., & Leder, P. (1981) *J. Biol. Chem.* **256**, 5116–5120.
22. Davis, R. W., Simon, M. & Davidson, N. (1971) *Methods Enzymol.* **21**, 413–428.
23. Maxam, A. M. & Gilbert, W. (1980) *Methods Enzymol.* **65**, 499–560.
24. Tu, C. D. & Cohen, S. N. (1980) *Gene* **10**, 177–183.
25. Boseley, P. G., Moss, T. & Birnstiel, M. L. (1980) *Methods Enzymol.* **65**, 478–494.
26. Rigby, P. W., Dieckmann, M., Rhodes, C. & Berg, P. (1977) *J. Mol. Biol.* **113**, 237–251.
27. Seed, B. (1982) *Nucleic Acids Res.* **10**, 1799–1810.
28. Alwine, J. C., Kemp, D. J., Parker, B. A., Reiser, J., Renart, J., Stark, G. R. & Wahl, G. M. (1979) *Methods Enzymol.* **68**, 220–242.
29. deWet, J. R., Daniels, D. L., Schroeder, J. L., Williams, B. G., Denniston-Thompson, K., Moore, D. D. & Blattner, F. R. (1980) *J. Virol.* **33**, 401–410.
30. Rimm, D. L., Horness, D., Kucera, J. & Blattner, F. R. (1980) *Gene* **12**, 301–309.
31. Shen-Ong, G. L. C. & Cole, M. D. (1982) *J. Virol.* **42**, 411–421.
32. Cole, M. D., Ono, M. & Huang, R. C. (1981) *J. Virol.* **38**, 680–687.
33. Varmus, H. E. (1982) *Science* **216**, 812–820.
34. Breathnach, R. & Chambon, P. (1981) *Annu. Rev. Biochem.* **50**, 349–383.
35. Proudfoot, N. J. & Brownlee, G. C. (1974) *Nature (London)* **252**, 359–362.
36. Benoist, C., O'Hare, K., Breathnach, R. & Chambon, P. (1980) *Nucleic Acids Res.* **8**, 127–142.
37. Cole, M. D., Ono, M. & Huang, R. C. (1982) *J. Virol.* **42**, 123–130.
38. Swanstrom, R., deLorbe, W., Bishop, J. M. & Varmus, E. (1981) *Proc. Natl. Acad. Sci. USA* **78**, 124–128.
39. Shapiro, J. (1979) *Proc. Natl. Acad. Sci. USA* **76**, 1933–1937.
40. Calos, M. P. & Miller, J. H. (1980) *Cell* **20**, 579–595.